

# Poly(triarylamine): Its Synthesis, Properties, and Blend with Polyfluorene for White-Light Electroluminescence

HUNG-YI LIN,<sup>1</sup> GUEY-SHENG LIOU,<sup>1</sup> WEN-YA LEE,<sup>2</sup> WEN-CHANG CHEN<sup>2</sup>

<sup>1</sup>Functional Polymeric Materials Research Laboratory, Department of Applied Chemistry, National Chi Nan University, Nantou Hsien, Taiwan, 545, Republic of China

<sup>2</sup>Optoelectronic Polymers Laboratory, Department of Chemical Engineering, National Taiwan University, Taipei, Taiwan, 106, Republic of China

Received 6 November 2006; accepted 8 December 2006

DOI: 10.1002/pola.21940

Published online in Wiley InterScience (www.interscience.wiley.com).

**ABSTRACT:** A new high-molecular-weight poly(triarylamine), poly[di(1-naphthyl)-4-anisylamine] (PDNAA), was successfully synthesized by oxidative coupling polymerization from di(1-naphthyl)-4-anisylamine (DNAA) with FeCl<sub>3</sub> as an oxidant. PDNAA was readily soluble in common organic solvents and could be processed into freestanding films with high thermal decomposition and softening temperatures. Cyclic voltammograms of DNAA and PDNAA exhibited reversible oxidative redox couples at the potentials of 0.85 and 0.85 V, respectively, because of the oxidation of the main-chain triarylamine unit. This suggested that PDNAA is a hole-transporting material with an estimated HOMO level of 5.19 eV. The absorption maximum of a PDNAA film appeared at 370 nm, with an estimated band gap of 2.86 eV from the absorption edge. Unusual multiple photoluminescence maxima were observed at 546 nm, and this suggested its potential application in white-light-emission devices. Nearly white-light-emission devices could be obtained with either a bilayer-structure approach [indium tin oxide/poly(ethylenedioxythiophene):poly(styrene sulfonate)/PDNAA/poly[2,7-(9,9-dihexylfluorene)] (PF)/Ca] or a polymer-blend approach (PF/PDNAA = 95:5). The luminance yield and maximum external quantum efficiency of the light-emitting diode with the PF/PDNAA blend as the emissive layer were 1.29 cd/A and 0.71%, respectively, and were significantly higher than those of the homopolymer. This study suggests that the PDNAA is a versatile material for electronic and optoelectronic applications. © 2007 Wiley Periodicals, Inc. *J Polym Sci Part A: Polym Chem* 45: 1727–1736, 2007

**Keywords:** electrochemistry; fluorescence; functionalization of polymers; high temperature materials; light-emitting diodes (LED)

## INTRODUCTION

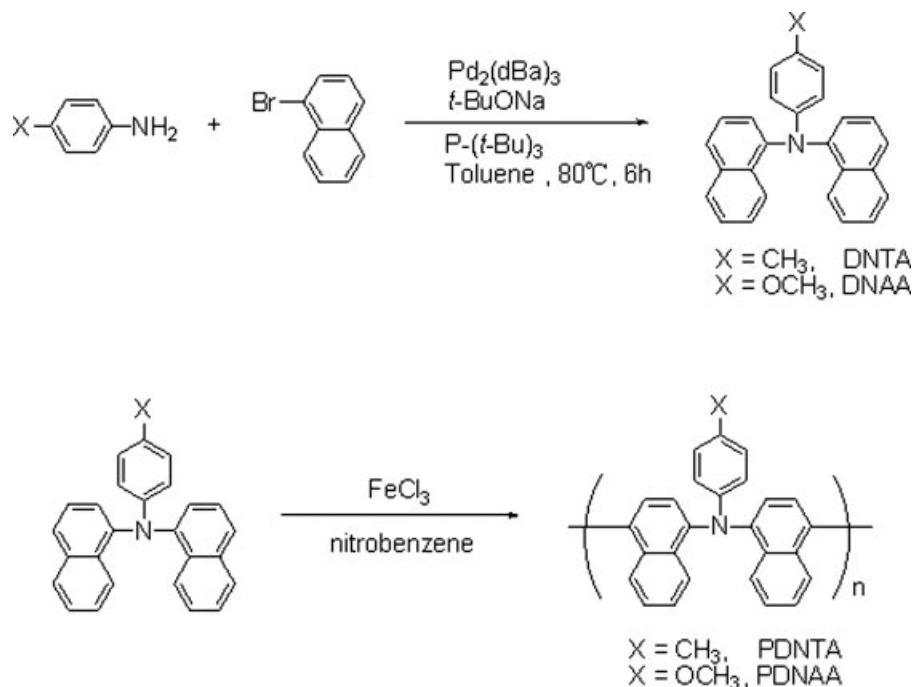
Triarylaminines have attracted considerable interest because of their excellent hole-transport characteristics for various organic electronic and optoelectronic devices, such as light-emitting diodes, field effect transistors, solar cells, and electro-

chromic devices.<sup>1,2</sup> However, small molecules or oligomers containing triarylaminines easily crystallize and require complicated vacuum deposition equipment for processing into thin films, and this limits their device applications. Such limitations have stimulated significant interest in developing polymers containing triarylamine units.

Various synthetic approaches have been developed to synthesize organics with triarylamine in the main-chain unit, including Ullman reactions,<sup>3</sup> palladium<sup>4,5</sup> or nickel-catalyzed coupling reactions,<sup>6</sup> and

Correspondence to: G.-S. Liou (E-mail: gsliou@ncnu.edu.tw) or W.-C. Chen (E-mail: chenwc@ntu.edu.tw)

*Journal of Polymer Science: Part A: Polymer Chemistry*, Vol. 45, 1727–1736 (2007)  
© 2007 Wiley Periodicals, Inc.



**Scheme 1.** Synthesis of monomers and polymers.

nucleophilic substitution reactions.<sup>7</sup> However, this has led to products with poor solubility and lower molecular weights. One of the first successful examples was developed by Ogino et al.,<sup>8</sup> who reported the oxidative coupling polymerization of 4-methyltriphenylamine with  $\text{FeCl}_3$  as an oxidant for the synthesis of poly(triarylamine). Although it is a simple and straightforward methodology for preparing polymeric triarylamine without introducing extra leaving and nucleophilic groups on the monomers, it suffers the major defect of low molecular weights. Recently, Ueda et al.<sup>9</sup> discovered a novel thermally stable hole-transporting polymer, poly[di(1-naphthyl)-4-tolylamine] (PDNTA), based on the oxidative coupling polymerization of triarylamine monomer di(1-naphthyl)-4-tolylamine (DNTA) with  $\text{FeCl}_3$  as the oxidant. Organic light-emitting diodes with PDNTA as a hole-transporting layer have shown excellent luminescence characteristics. Although poly(triarylamine)s are generally regarded as hole-transporting materials, organic light-emitting diode devices using them as active layers have rarely been explored because of the low quantum yield of such polymers.

In this article, the synthesis and characterization of a novel aromatic poly(triarylamine), poly[di(1-naphthyl)-4-anisylamine] (PDNAA), are reported. It was synthesized with a new monomer, di(1-naphthyl)-4-anisylamine (DNAA), with  $\text{FeCl}_3$  as an oxidant, as shown in Scheme 1. The prepared PDNAA had a

high molecular weight and exhibited excellent solubility and thermal properties. The electrochemical and photoluminescence (PL) properties of the polymer were prepared via the casting of a solution onto an indium tin oxide (ITO) coated glass substrate. Light-emitting diode devices [ITO/poly(ethylenedioxythiophene):poly(styrene sulfonate) (PEDOT:PSS)/active layer/Ca/Ag structure] using the bilayer structure of PDNAA/poly[2,7-(9,9-dihexylfluorene)] (PF) or a PF/PDNAA blend exhibited significantly enhanced luminescence characteristics over the PF single layer.<sup>10,11</sup> Besides, unusual white-light electroluminescence (EL) was discovered based on PDNAA. This study opens new applications of poly(triarylamine)s for organic light-emitting diode devices.

## EXPERIMENTAL

### Materials

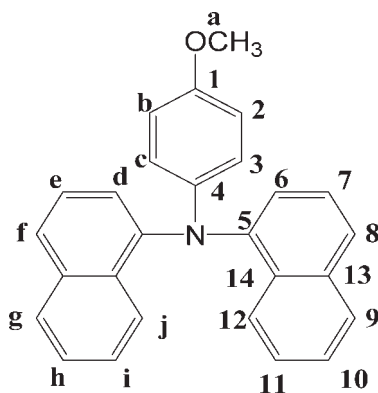
DNTA (mp = 155–157 °C) was obtained by the palladium-catalyzed N-arylation reaction of *p*-toluidine with 2 equiv of 1-bromonaphthalene, as shown in Scheme 1, according to a previously reported procedure.<sup>9</sup> *p*-Anisidine (Alfa Aesar; 98%), *p*-toluidine (Acros; 98%), 1-bromonaphthalene (Acros; 98%), tris(dibenzylideneacetone) dipalladium (Lancaster), tri-*tert*-butyl phosphine, sodium *tert*-butoxide (Acros), iron(III) chloride

(Showa), and nitrobenzene (Tedia) were acquired. Tetrabutylammonium perchlorate (TBAP) was obtained from Acros and recrystallized twice from ethyl acetate and then dried *in vacuo* before use. The solvents and other reagents were used as received from commercial suppliers. PF was synthesized according to our previous publication.<sup>12</sup>

### Synthesis of the Monomer: DNAA

To a three-necked flask equipped with a reflux condenser, 1-bromonaphthalene (6.833 g, 33 mmol), *p*-anisidine (1.847 g, 15 mmol), Pd<sub>2</sub>(dba)<sub>3</sub> (0.340 g, 0.33 mmol), P(*t*-Bu)<sub>3</sub> (0.357 g, 1.32 mmol), *tert*-BuONa (4.440 g, 46.2 mmol), and toluene (30 mL) were added and stirred at 80 °C until *p*-anisidine disappeared in TLC analysis. The precipitate was removed, and the filtrate was concentrated on a rotary evaporator. The residue was extracted with ethyl acetate and dried over MgSO<sub>4</sub> and then was concentrated under reduced pressure. The product was recrystallized from a methanol/isopropyl alcohol and H<sub>2</sub>O mixture, affording a brownish solid with a yield of 3.206 g (56%).

mp: 182–187 °C [differential scanning calorimetry (DSC) at a scanning rate of 10 °C/min]. IR (KBr)  $\nu$ : 3046 (Ar C—H), 2915, 2857 (C—H stretch), 1570, 1503 (C=C), 1391 (C—N), 1240, 1035 (aromatic —C—O—C— stretch), 775 cm<sup>-1</sup> (naphthalene-H). <sup>1</sup>H NMR (300 MHz CDCl<sub>3</sub>,  $\delta$ , ppm): 8.07 (d, 2H, H<sub>j</sub>), 7.87 (d, 2H, H<sub>g</sub>), 7.65 (d, 2H, H<sub>f</sub>), 7.46 (t, 2H, H<sub>h</sub>), 7.35 (t, 2H, H<sub>e</sub>), 7.31 (d, 2H, H<sub>i</sub>), 7.11 (d, 2H, H<sub>d</sub>), 6.79 (d, 2H, H<sub>b</sub>), 6.74 (d, 2H, H<sub>c</sub>), 3.75 (s, 3H, H<sub>a</sub>). <sup>13</sup>C NMR (CDCl<sub>3</sub>,  $\delta$ , ppm): 154.5 (C<sup>1</sup>), 145.7 (C<sup>5</sup>), 144.4 (C<sup>4</sup>), 135.2 (C<sup>13</sup>), 129.8 (C<sup>14</sup>), 128.3 (C<sup>9</sup>), 126.0 (C<sup>7</sup>), 125.9 (C<sup>10</sup>), 125.9 (C<sup>11</sup>), 124.9 (C<sup>8</sup>), 124.4 (C<sup>6</sup>), 124.0 (C<sup>12</sup>), 123.1 (C<sup>2</sup>), 114.3 (C<sup>3</sup>). ELEM. ANAL. calcd for C<sub>27</sub>H<sub>21</sub>NO (375.46): C, 86.37%; H, 5.64%; N, 3.73%. Found: C, 86.23%; H, 5.60%; N, 3.63%.



### Polymer Synthesis

A typical example of the polymerization was as follows: In a 50-mL, round-bottom flask fitted with a three-way stopcock were placed DNAA (0.375 g, 1.0 mmol), FeCl<sub>3</sub> (0.404 g, 2.5 mmol), and nitrobenzene (2 mL) under nitrogen. The solution was stirred at room temperature for 24 h and poured into a mixture of methanol containing 10% hydrochloric acid. The precipitate was collected and washed thoroughly with aqueous ammonium hydroxide. Precipitations from chloroform into methanol was carried out twice for further purification to afford 0.30 g of the polymer (yield = 80%).

IR (KBr)  $\nu$ : 3047 (Ar C—H), 2915, 2856 (C—H stretch), 1576, 1505 (C=C), 1376 (C—N), 1245, 1038 (aromatic —C—O—C— stretch), 758 cm<sup>-1</sup> (naphthalene-H). <sup>1</sup>H NMR (300 MHz CDCl<sub>3</sub>,  $\delta$ , ppm): 8.20 (d, 2H, H<sub>j</sub>), 7.60–7.18 (H<sub>d</sub> + H<sub>e</sub> + H<sub>g</sub> + H<sub>h</sub> + H<sub>i</sub>), 6.91 (d, 2H, H<sub>b</sub>), 6.88 (d, 2H, H<sub>c</sub>), 3.74 (s, 3H, H<sub>a</sub>). <sup>13</sup>C NMR (CDCl<sub>3</sub>,  $\delta$ , ppm): 154.5 (C<sup>1</sup>), 145.4 (C<sup>5</sup>), 144.5 (C<sup>4</sup>), 135.3 (C<sup>13</sup>), 134.6 (C<sup>8</sup>), 129.9 (C<sup>14</sup>), 128.3 (C<sup>9</sup>), 127.7 (C<sup>7</sup>), 127.2 (C<sup>10</sup>), 125.9 (C<sup>11</sup>), 124.7 (C<sup>6</sup>), 123.8 (C<sup>12</sup>), 123.1 (C<sup>2</sup>), 114.5 (C<sup>3</sup>). ELEM. ANAL. calcd for (C<sub>27</sub>H<sub>19</sub>NO)<sub>n</sub> (373.45): C, 86.84%; H, 5.13%; N, 3.75%. Found: C, 86.73%; H, 5.09%; N, 3.62%.

### Preparation of the Films

A polymer solution was made by the dissolution of about 0.3 g of the polymer sample in 5 mL of DMAc. The homogeneous solution was poured into a 3-cm glass Petri dish, which was placed in a 90 °C oven overnight for the slow release of the solvent, and then the film was stripped off from the glass substrate and further dried *in vacuo* at 150 °C for 8 h. The obtained films were used for measurements of the molecular weights, solubility, and thermal properties and electrochemical analyses.

### Measurements

IR spectra were recorded on a PerkinElmer RXI FTIR spectrometer. Elemental analyses were run in an Elementar VarioEL-III. <sup>1</sup>H and <sup>13</sup>C NMR spectra were measured on a Bruker AV-300 FT-NMR system. Ultraviolet–visible (UV–vis) spectra of the polymer films were recorded on a Varian Cary 50 Probe spectrometer. Thermogravimetric analysis (TGA) was conducted with a Perkin Elmer Pyris 1 thermogravimetric analyzer. Ex-

periments were carried out on approximately 6–8-mg film samples heated in flowing nitrogen or air (flow rate = 20 cm<sup>3</sup>/min) at a heating rate of 20 °C/min. DSC analyses were performed on a PerkinElmer Pyris Diamond differential scanning calorimeter at a scanning rate of 20 °C/min in flowing nitrogen (20 cm<sup>3</sup>/min). Thermomechanical analysis (TMA) was conducted with a PerkinElmer TMA 7 instrument. The TMA experiments were conducted from 50 to 350 °C at a scanning rate of 10 °C/min with a penetration probe 1.0 mm in diameter under an applied constant load of 10 mN.

Electrochemistry was performed with a Bioanalytical System model CV-27 potentiostat and a BAS X-Y recorder. Cyclic voltammetry was conducted with the use of a three-electrode cell in which glass carbon (GC) was used as a working electrode. A platinum wire was used as an auxiliary electrode. All cell potentials were taken with a home-made Ag/AgCl, KCl (saturated) reference electrode. Absorption spectra in spectroelectrochemical analysis were measured with an HP 8453 UV-vis spectrophotometer. PL spectra were measured with a Jasco FP-6300 spectrofluorometer. The fluorescence quantum yields ( $\Phi_F$ ) of the samples were measured with quinine sulfate in 1 N H<sub>2</sub>SO<sub>4</sub> as a reference standard ( $\Phi_F = 0.546$ ).<sup>13</sup>

### Device Fabrication and Testing

The EL devices were fabricated on ITO-coated glass substrates with a sheet resistance of 20–30 Ω/sq. The substrate was ultrasonically cleaned with detergent, deionized water, acetone, and methanol subsequently. On the ITO glass, a layer of PEDOT:PSS, 50–60 nm thick (probed with an Alpha-Step 500 surface profiler), was formed through spin coating from its aqueous solution (Baytron P 8000, Bayer). The single-layer emissive layer was spin-coated at 2000 rpm from the corresponding CHCl<sub>3</sub> solution (1.5 wt %) on top of the vacuum-dried PEDOT:PSS layer; the bilayer polymeric light-emitting diode device was first spin-coated on an ITO glass from a PDNAA solution in CHCl<sub>3</sub>. The spin-coated PDNAA layer was dried at 80 °C, and then PF was spin-coated onto the surface of the PDNAA films from a PF cyclohexane solution. The nominal thickness of the emissive layer was 60–70 nm. Under a base pressure below  $2 \times 10^{-4}$  Torr, a layer of Ca (10 nm) was vacuum-deposited as a cathode, and a thick layer of Ag (100 nm) was deposited subsequently as a protecting layer. The cathode area defined the

active area of the device, which was 0.1256 cm<sup>2</sup> in this study. Current–voltage characteristics were measured with a computerized Keithley 2400 source measure unit. The luminance and Commission Internationale de l'Eclairage (CIE) coordinates of the device were measured with a Konica–Minolta CS-100A chromameter. The EL spectrum of the device was recorded on a Fluorolog-3 spectrofluorometer (Jobin Yvon).

## RESULTS AND DISCUSSION

### Monomer Synthesis

The monomer DNAA was synthesized by the palladium-catalyzed N-arylation reaction of *p*-anisidine with 2.0 equiv of 1-bromonaphthalene, as shown in Scheme 1. The product was purified by recrystallization from a methanol/isopropyl alcohol and H<sub>2</sub>O mixture to give a brownish solid. Elemental analysis and IR, <sup>1</sup>H NMR, and <sup>13</sup>C NMR spectroscopy techniques were used to identify the chemical structures of DNAA.

The characteristic IR spectrum of DNAA shown in Figure 1 presents absorption peaks at 1570 and 1503 cm<sup>-1</sup> (the C=C bond of the aromatic rings) and at 1391 cm<sup>-1</sup> (C–N). No absorption bands due to the NH<sub>2</sub> stretching of *p*-anisidine around 3420 and 3340 cm<sup>-1</sup> can be observed in Figure 1. Figure 2 illustrates the <sup>1</sup>H and <sup>13</sup>C NMR spectra of DNAA. A full assignment of the aromatic protons was required to determine the coupling position between naphthyl units. Figure 3 shows the H–H COSY spectrum for the aro-

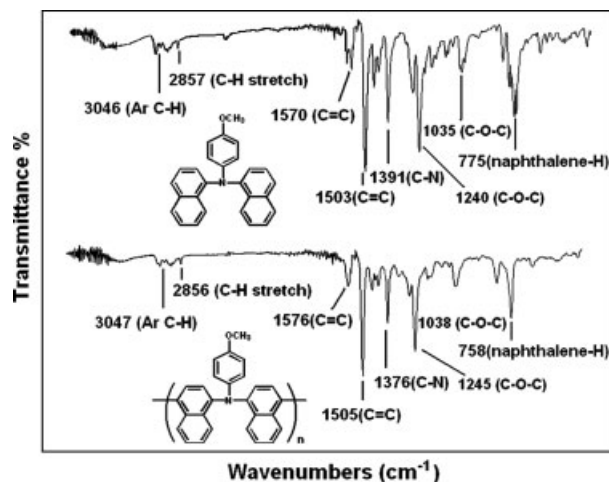


**Figure 1.** FTIR spectra of DNAA and PDNAA.

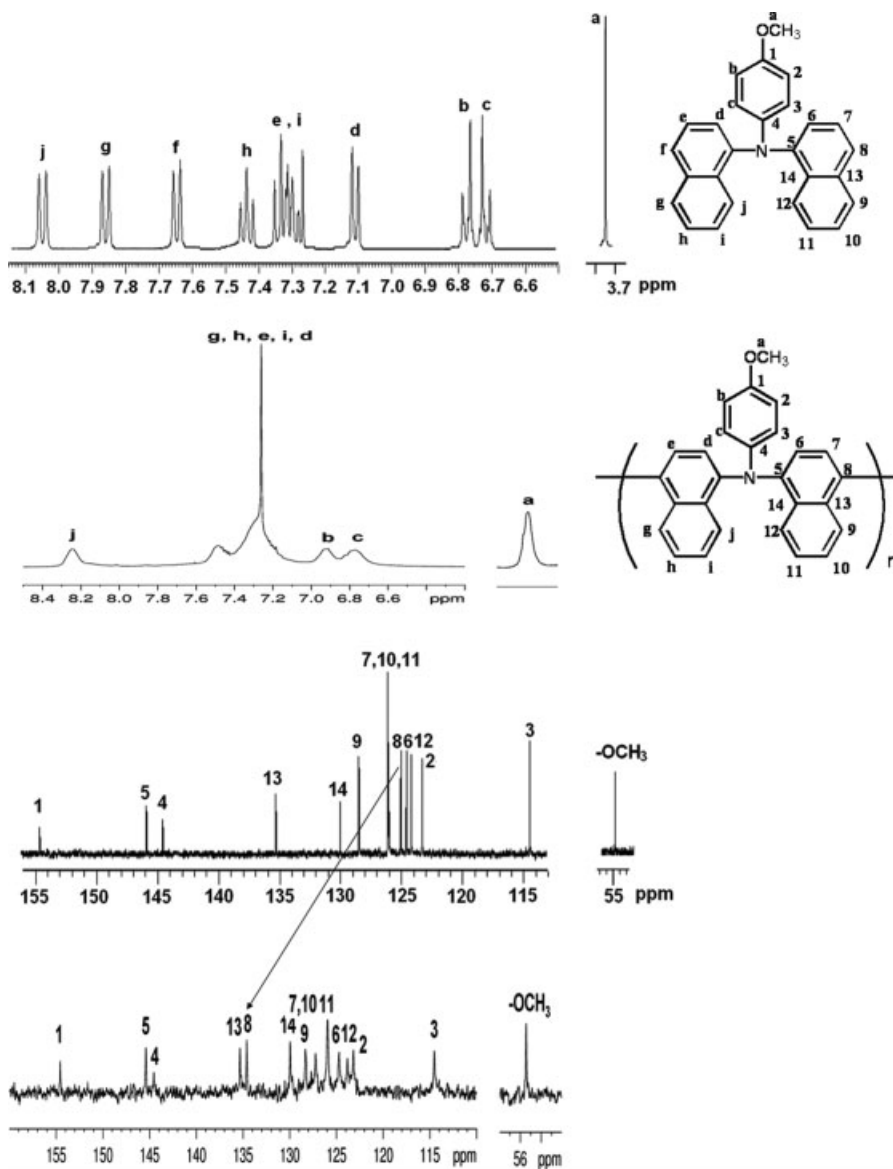


**Figure 2.**  $^1\text{H}$  and  $^{13}\text{C}$  NMR spectra of DNAA and PDNAA in  $\text{CDCl}_3$ .

matic region of DNAA. Aromatic signals at 6.79 and 6.74 ppm are connected with a singlet signal at 3.75 ppm. These signals can be assigned to the aromatic protons of the anisylamino unit. Accordingly, the resonances at 8.07 and 7.87 ppm of DNAA are assigned to the protons at positions j and g, respectively. Because the signals at 6.79 and 6.74 ppm have been assigned to the protons at positions b and c, the signal at 7.11 ppm is assigned to the proton at position d. The proton at position g is connected to a triplet signal at 7.46 ppm, and this indicates that this triplet signal is due to the proton at position h. Other doublet and triplet signals at 7.65 and 7.35–7.31 ppm are assigned to the protons at positions f and e and i,

respectively. All assignments of aromatic protons are summarized in Figure 3. Further spectral evidence for DNAA is given by  $^{13}\text{C}$  NMR and C–H COSY spectroscopy. There are 15 resonance signals in the  $^{13}\text{C}$  NMR spectrum of DNAA due to one methoxyl carbon and 14 aromatic carbons. In the aromatic region, five resonance peaks at 154.5, 145.7, 144.4, 135.2, and 129.8 ppm are peculiar to quaternary carbons. The other aromatic  $^{13}\text{C}$  signals are well connected to the corresponding protons, as shown in the C–H COSY spectrum (Fig. 4). The elemental analysis of C, H, and N also shows excellent agreement with the theoretical contents. These results suggest the successful synthesis of the monomer DNAA.

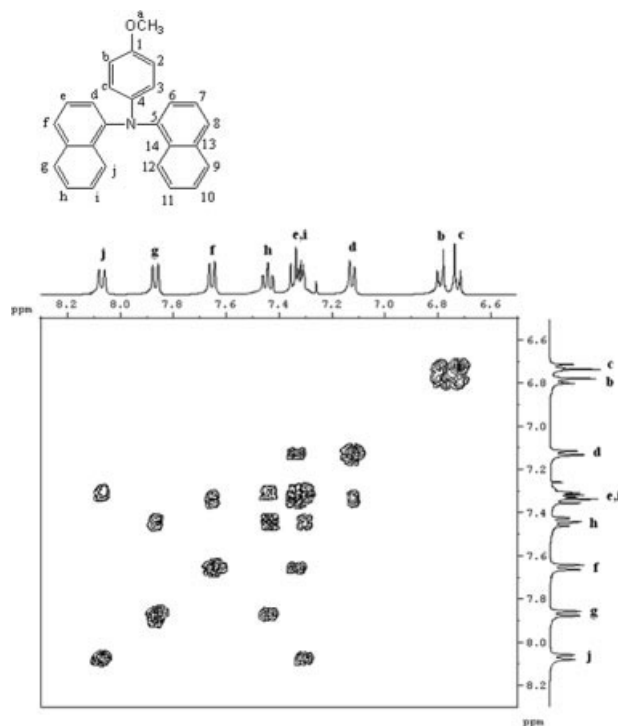


**Figure 3.** H-H COSY spectrum of DNAA in  $\text{CDCl}_3$ .

### Polymer Synthesis

PDNAA could be readily prepared by the oxidative coupling polymerization of DNAA with  $\text{FeCl}_3$  as an oxidant. The structure of the polymer was confirmed by IR and  $^1\text{H}$  and  $^{13}\text{C}$  NMR spectroscopy, as shown in Figures 1 and 2, respectively. The molecular weight of PDNAA was measured by GPC with polystyrenes as standards and THF as an eluent, and the weight-average molecular weight and polydispersity index were determined to be 30,000 and 1.41, respectively. The polymer also showed excellent solubility in common organic solvents such as chloroform and THF (Table 1) and could readily be cast into a pale yellow, freestanding film. This suggests that the introduction of the 4-methoxyphenyl group into the polymer backbone increases the solubility and processibility of the triarylamine-containing polymer.

### Thermal Properties

DSC, TMA, and TGA were used to evaluate the thermal properties of PDNAA. The results are summarized in Table 1. The DSC curve exhibits no endothermic peak or baseline shift due to the melting point and glass transition, respectively, but the softening temperature ( $186^\circ\text{C}$ ) of PDNAA

was observed by TMA with a loaded penetration probe, as illustrated in Figure 5. As revealed by the TGA measurements, PDNAA exhibited good thermal stability with a 10% weight loss temperature in excess of  $547^\circ\text{C}$  and a char yield at  $800^\circ\text{C}$  higher than 69% in nitrogen.

### Electrochemical Properties

The redox behavior was investigated by cyclic voltammetry conducted with GC as a working electrode in dry dichloromethane ( $\text{CH}_2\text{Cl}_2$ ) containing 0.1 M TBAP as an electrolyte under a nitrogen atmosphere. Figure 6 shows the cyclic voltammograms of DNAA and PDNAA with a clear reversible oxidation redox  $E_{\text{onset}}$  at 0.85 and 0.85 V, respectively, even after over 300 cyclic scans. This suggests that PDNAA has excellent stability with respect to its electrochemical characteristics. The HOMO energy level of PDNAA has been determined from the oxidation onset potentials. The oxidation onset potential for PDNAA has been determined to be 0.85 V versus Ag/AgCl. The external ferrocene/ferrocenium ( $\text{Fc}/\text{Fc}^+$ ) redox standard  $E_{1/2}$  is 0.46 V versus Ag/AgCl in  $\text{CH}_2\text{Cl}_2$ . Assuming that the HOMO energy for the  $\text{Fc}/\text{Fc}^+$  standard is 4.80 eV with respect to the zero vacuum level, the HOMO energy level for PDNAA has been estimated to be 5.19 eV. For comparison,

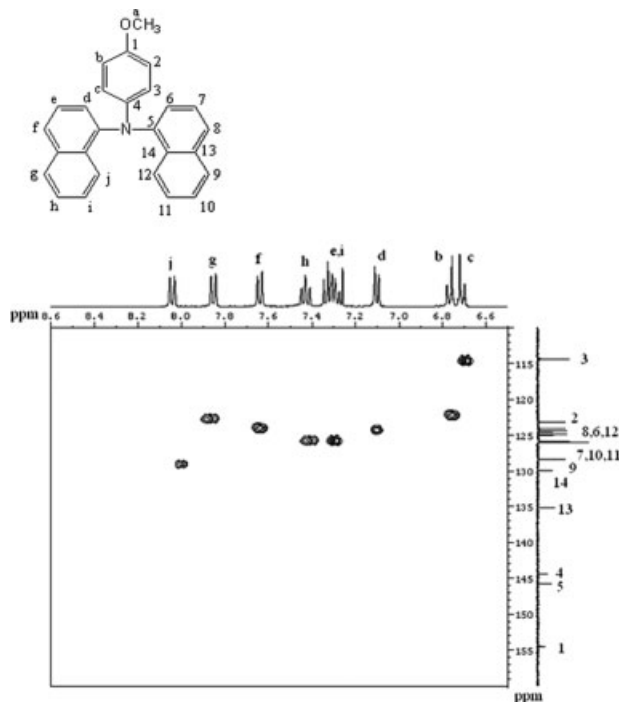


**Figure 4.** C-H HMQC spectrum of DNAA in  $\text{CDCl}_3$ .

**Table 1.** Molecular Weights, Thermal Properties, and Solubility of PDNTA and PDNAA

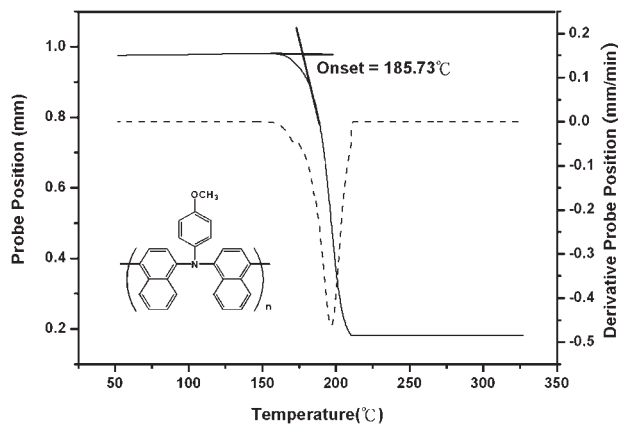
Polymer Code	$M_w^a$	$M_n^a$	$M_w/M_n^a$	$T_{d,5\%}^b$		$T_{d,10\%}^c$		Char Yield (wt %) at 800 °C in N <sub>2</sub>	Solubility <sup>d</sup>							
				In N <sub>2</sub>	In Air	In N <sub>2</sub>	In Air		CHCl <sub>3</sub>	THF	NMP	DMF	DMAC	DMSO		
PDNTA	29,500	21,000	1.39	544	434	582	454	74	++	++	++	-	-	+	-	-
PDNAA	30,000	21,500	1.41	517	419	547	430	69	++	++	++	-	-	+	+	-

<sup>a</sup> Average molecular weights with respect to a polystyrene standard in THF by GPC.

<sup>b</sup> Decomposition temperature at which a 5% weight loss was recorded by TGA at a scanning rate of 20 °C/min.

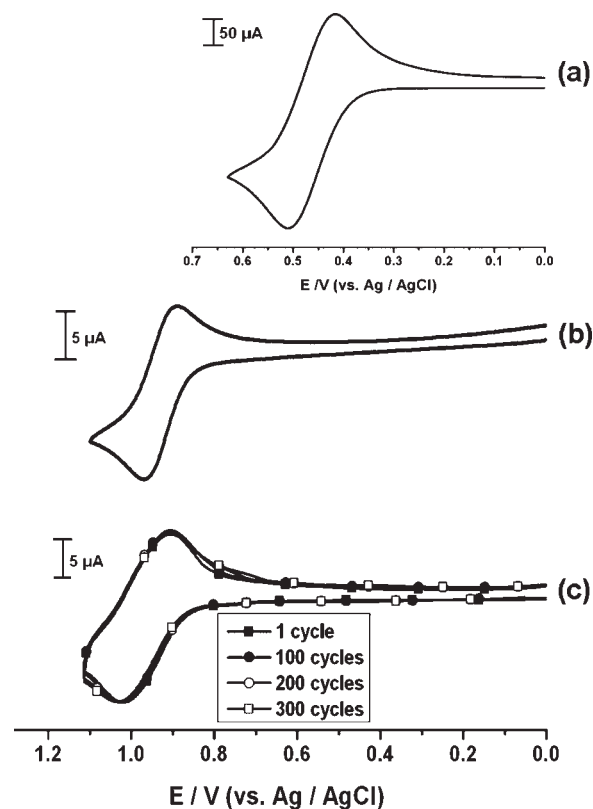
<sup>c</sup> Decomposition temperature at which a 10% weight loss was recorded by TGA at a scanning rate of 20 °C/min.

<sup>d</sup> ++ = soluble at room temperature; + = soluble on heating; - = insoluble even on heating.






**Figure 5.** TMA curve for PDNAA (heating rate = 10 °C/min; applied force = 10 mN).

the cyclic voltammetry of PDNTA has also been studied, and it has been estimated to have a HOMO energy level of 5.28 eV (Table 2). Hence, the replacement of the methyl substituent by the more electron-donating methoxy group not only increases the HOMO energy level but also stabilizes the oxidized form of the polymer.



**Figure 6.** Cyclic Voltammograms of (a) ferrocene (b) DNAA (c) PDNAA in CH<sub>2</sub>Cl<sub>2</sub> containing 0.1 M TBAP. Scan rate = 0.05 V/s.

**Table 2.** Optical and Electrochemical Properties of PDNTA and PDNAA

Polymer Code	Color of the Film <sup>a</sup>	Solution Wavelength (nm) <sup>b</sup>			Film Wavelength (nm) <sup>b</sup>			$E_{\text{onset}}$ (V)	$E_{\text{g}}$ (eV) <sup>d</sup>	HOMO (eV) <sup>e</sup>	LUMO (eV) <sup>f</sup>
		Absorption Maximum	Absorption Onset	PL Maximum	$\Phi_{\text{F}}$ (%) <sup>c</sup>	Absorption Maximum	Absorption Onset				
DNTA		353	388	449	17	—	—	0.95	—	5.29	—
PDNTA		364	392	462	13	364	533	0.94	2.91	5.28	2.37
DNAA		347	408	465	12	—	—	0.85	—	5.19	—
PDNAA		363	411	478	10	370	546	0.85	2.86	5.19	2.33

<sup>a</sup> The photographs show the appearance of the polymer films.

<sup>b</sup> The UV-vis absorption measurements were taken at  $1 \times 10^{-5}$  M in NMP at room temperature.

<sup>c</sup> These values were measured with quinine sulfate [dissolved in 1 N H<sub>2</sub>SO<sub>4</sub> (aqueous)] at a concentration of  $10^{-5}$  M, assumed to have  $\Phi_{\text{F}} = 0.546$ , as a standard at 24–25 °C. The excitation wavelength was  $\lambda_{\text{max}}$  for these solutions, which had absorbance of less than 0.05.

<sup>d</sup> The data were calculated with the following equation: Gap =  $1240/\lambda_{\text{onset}}$ .

<sup>e</sup> The HOMO energy levels were calculated from cyclic voltammetry and were referenced to ferrocene (4.8 eV).

<sup>f</sup> LUMO = HOMO – Gap.

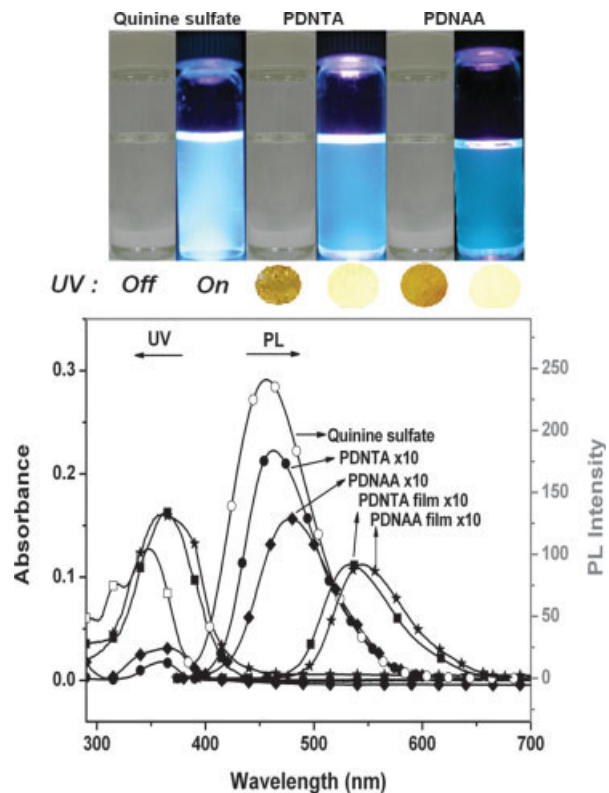


**Figure 7.** UV-Vis absorption and photoluminescence spectra of PDNTA and PDNAA in NMP solution and solid state film. Solution and thin film of PDNTA and PDNAA were excited by UV irradiation at 365 nm.

### Optical Absorption and PL Properties

The UV-vis absorption and PL spectra of PDNAA were investigated in a dilute solution ( $10^{-5}$  M) of NMP and in a thin-film state at room temperature (Fig. 7); the results are listed in Table 2.

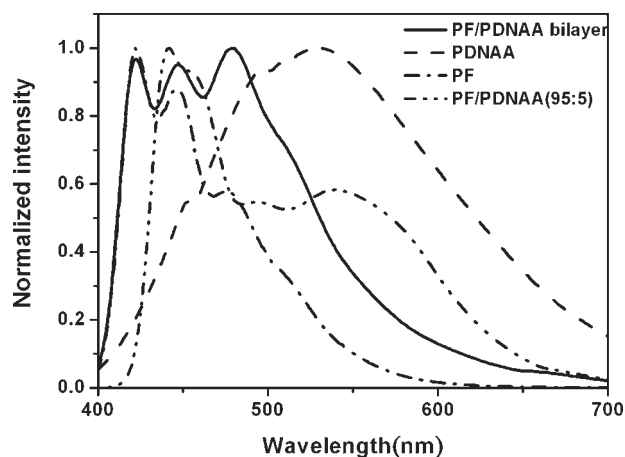


**Figure 8.** Electroluminescence spectra of PDNAA, PF, PF/PDNAA bilayer, and PF/PDNAA (95:5) blend.



**Table 3.** EL Characteristics with PF, PDNAA, PF/PDNAA Bilayer, and PF/PDNAA Blend (95:5) Active Layers

Active Layer	Bias (V)	Emission $\lambda_{\max}$ (nm)	CIE (x, y)	Brightness (cd/m <sup>2</sup> )	Luminance Yield (cd/A)	EQE (%) <sup>a</sup>
PF	10	422, 446, 477	0.179, 0.186	184	0.218	0.22
PDNAA	26	529	0.447, 0.497	31.6	0.014	0.01
PF/PDNAA bilayer	32	422, 447, 479	0.300, 0.372	215	0.120	0.08
PF/PDNAA blend (95:5)	27.5	429, 447, 524	0.299, 0.384	2600	1.290	0.71

<sup>a</sup> External quantum efficiency.

Figure 7 shows the UV–vis absorption and PL spectra of PDNTA and PDNAA, respectively. The absorption maxima of PDNAA in the NMP solution and solid-state film can be observed at 363 and 370 nm, respectively, with an onset of 433 nm. The estimated optical band gap of the PDNAA is around 2.86 eV, which is close to that of PDNTA reported in the literature.<sup>9</sup> PDNAA in the NMP solution exhibited a maximum blue fluorescence peak at 478 nm with a quantum efficiency of 10% in comparison with that of quinine sulfate. However, luminescence peaks at 546 nm were found for the solid-state films. Such a vibrational-structure-like emission probably occurs because the polymer geometry becomes more coplanar in the excited state.<sup>14</sup> It also indicates that the coplanar geometry of triarylamine units is probably induced in the solid-state film of PDNAA. The multiple luminescence peaks suggest the potential applications of PDNAA for white-light-emission devices.

### Device Fabrication and EL Properties

The EL spectra of devices based on PF, PDNAA, PF/PDNAA, and PF/PDNAA (95:5), shown in Figure 8, have emission maxima at (422, 446, 477), 529, (422, 447, 479), and (429, 447, 524), respectively. A comparison of the shapes of the spectra shows that the PF/PDNAA bilayer is an intermediate between the homopolymers of PF and PDNAA, but the PF/PDNAA blend is a superimposition of PF and PDNAA. Because there is no significant overlap between the PL of PF and the absorption of PDNAA, Forster energy transfer probably does not occur in this case, and this explains the EL spectra of the bilayer or blend. However, such multiple emissions could be important for white-light-emitting diodes because their emission spectra cover all of the visible range. As shown in Table 3, the CIE 1931 coordinates of the

polymer bilayer and blend devices are (0.300, 0.372) and (0.299, 0.384), which are close to those of the pure white-light emission of (0.33, 0.33). The brightness (cd/m<sup>2</sup>), luminescence yield (cd/A), and external quantum yield (%) of the PF/PDNAA bilayer and polymer blend based devices are (215, 0.120, 0.08) and (2600, 1.290, 0.71), respectively, as shown in Table 3. The luminance yield and external quantum efficiency of the bilayer device are smaller than those of the PF device. This is probably due to the relatively low luminescence yield (0.014 cd/A) and external quantum efficiency (0.01%) of PDNAA. The luminance intensity of the PDNAA/PF bilayer device could be higher than that of PF because the electron-transporting barrier at the PDNAA/PF interface increases the exciton recombination efficiency of the emitting layer. Note that the electron affinities of PF and PDNAA are 2.44<sup>12</sup> and 2.33 eV (estimated from the difference between the optical band gap of 2.86 eV and the HOMO level of 5.19 eV), respectively, and thus an electron-transporting barrier of 0.11 eV exists on the interface. However, the EL characteristics of the device based on the PF/PDNAA (95:5) polymer blend are significantly higher than those of PF and PDNAA. The polymer blend probably has a much higher interface area between PF and PDNAA than the bilayer structure. Thus, the electron-blocking property of PDNAA in the blend significantly enhances the luminescence yield, which is about 6 times higher than that of the PF device. The multiple-emission and hole-transporting characteristics open another possible approach for achieving high-brightness white-light-emission devices.

### CONCLUSIONS

A new poly(triarylamine) (PDNAA) was successfully synthesized by oxidative coupling polymer-

ization with  $\text{FeCl}_3$  as an oxidant. It was very soluble in common organic solvents and exhibited high thermal stability. PDNAA is a hole-transporting material with an estimated HOMO level of 5.19 eV. The absorption maximum of the PDNAA film was found at 370 nm, with an estimated band gap of 2.86 eV from the absorption edge. Nearly white-light-emission devices could be obtained with either a bilayer-structure approach (ITO/PEDOT:PSS/PDNAA/PF/Ca) or polymer-blend approach (PF/PDNAA = 95:5). The luminance yield and maximum external quantum efficiency of the light-emitting diode with the PF/PDNAA blend as the emissive layer were 1.29 cd/A and 0.71%, respectively, and were significantly higher than those of their homopolymers. This study suggests that PDNAA is a versatile material for electronic and optoelectronic applications.

The authors are grateful to the National Science Council of the Republic of China for its financial support of this work.

## REFERENCES AND NOTES

- (a) Fang, Q.; Yamamoto, T. *Macromolecules* 2004, 37, 5894; (b) Shirota, Y. *J Mater Chem* 2005, 15, 79; (c) Wu, F. I.; Shi, P. I.; Shu, C. F.; Tang, Y. L.; Chi, Y. *Macromolecules* 2005, 38, 9028; (d) Sonntag, M.; Kreger, K.; Hanft, D.; Strohrigel, P.; Setayesh, S.; de Leeuw, D. *Chem Mater* 2005, 17, 3031; (e) Roquet, S.; Cravino, A.; Leriche, P.; Aleveque, O.; Frere, P.; Roncali, J. *J Am Chem Soc* 2006, 128, 3459; (f) Hawker, C. J.; Wooley, K. L. *Science* 2005, 309, 1200.
- (a) Cheng, S. H.; Hsiao, S. H.; Su, T. H.; Liou, G. S. *Macromolecules* 2005, 38, 307; (b) Liou, G. S.; Hsiao, S. H.; Chen, H. W. *J Mater Chem* 2006, 16, 1831; (c) Liou, G. S.; Yang, Y. L.; Su, Y. O. *J Polym Sci Part A: Polym Chem* 2006, 44, 2587; (d) Liou, G. S.; Huang, N. K.; Yang, Y. L. *J Polym Sci Part A: Polym Chem* 2006, 44, 4095; (e) Liou, G. S.; Hsiao, S. H.; Huang, N. K.; Yang, Y. L. *Macromolecules* 2006, 39, 5337; (f) Su, T. H.; Hsiao, S. H.; Liou, G. S. *J Polym Sci Part A: Polym Chem* 2005, 43, 2085.
- Thelakkat, M.; Hagen, J.; Haarer, D.; Schmidt, H. W. *Synth Met* 1999, 102, 125.
- Felix, E. G.; Sheila, I. H.; John, F. H. *J Am Chem Soc* 1999, 121, 7527.
- Yu, W. L.; Pei, J.; Huang, W.; Heeger, A. J. *Chem Commun* 2000, 681.
- Tanaka, S.; Iso, T.; Doke, Y. *Chem Commun* 1997, 2063.
- Kido, J.; Hamada, G.; Nagai, K. *Polym Adv Technol* 1996, 7, 31.
- Ogino, K.; Kanegae, A.; Yamaguchi, R.; Sato, H.; Kurjata, J. *Macromol Rapid Commun* 1999, 20, 103.
- Nomura, M.; Shibasaki, Y.; Ueda, M. *Macromolecules* 2004, 37, 1204.
- Kim, Y. H.; Zhao, Q.; Kwon, S. K. *J Polym Sci Part A: Polym Chem* 2006, 44, 172.
- Gong, X.; Moses, D.; Heeger, A. J. *J Phys Chem B* 2004, 108, 8601.
- Wu, W. C.; Liu, C. L.; Chen, W. C. *Polymer* 2006, 47, 527.
- Demas, J. N.; Crosby, G. A. *J Phys Chem* 1971, 75, 991.
- Lakowicz, J. R. *Principles of Fluorescence Spectroscopy*, 2nd ed.; Kluwer Academic/Plenum: Boston, 1999; pp 8–9.